Tumor and Stem Cell Biology

Cancer Research

ALDH1-Positive Cancer Stem Cells Predict Engraftment of Primary Breast Tumors and Are Governed by a Common Stem Cell Program

Emmanuelle Charafe-Jauffret[1,2,3], Christophe Ginestier[1], François Bertucci[1,3,4], Olivier Cabaud[1], Julien Wicinski[1], Pascal Finetti[1], Emmanuelle Josselin[1], José Adelaide[1], Tien-Tuan Nguyen[1], Florence Monville[1], Jocelyne Jacquemier[2], Jeanne Thomassin-Piana[2], Guillaume Pinna[7], Aurélie Jalaguier[6], Eric Lambaudie[5], Gilles Houvenaeghel[3,5], Luc Xerri[2,3], Annick Harel-Bellan[7], Max Chaffanet[1], Patrice Viens[1,3,4], and Daniel Birnbaum[1]

Abstract

Cancer stem-like cells (CSC) have been widely studied, but their clinical relevance has yet to be established in breast cancer. Here, we report the establishment of primary breast tumor–derived xenografts (PDX) that encompass the main diversity of human breast cancer and retain the major clinicopathologic features of primary tumors. Successful engraftment was correlated with the presence of ALDH1-positive CSCs, which predicted prognosis in patients. The xenografts we developed showed a hierarchical cell organization of breast cancer with the ALDH1-positive CSCs constituting the tumorigenic cell population. Analysis of gene expression from functionally validated CSCs yielded a breast CSC signature and identified a core transcriptional program of 19 genes shared with murine embryonic, hematopoietic, and neural stem cells. This generalized stem cell program allowed the identification of potential CSC regulators, which were related mainly to metabolic processes. Using an siRNA genetic screen designed to target the 19 genes, we validated the functional role of this stem cell program in the regulation of breast CSC biology. Our work offers a proof of the functional importance of CSCs in breast cancer, and it establishes the reliability of PDXs for use in developing personalized CSC therapies for patients with breast cancer. *Cancer Res; 73(24); 7290–300. ©2013 AACR.*

Introduction

Heterogeneity is a limitation to cure breast cancer, overcome recurrences and metastases (1). A major cause of heterogeneity is the hierarchical cellular organization: that endows a small, phenotypically distinct population of cancer stem cells (CSC) with the capacity to support tumor growth, metastasis and therapeutic resistance (2–11). Multiple pools of stem cells have been identified within a tumor by different means, including (12–14) mouse lineage tracing experiments (15–17). To measure the capacity of a subset of tumor cells to transfer a cancer, tumorigenesis assays with iso- or xenogenic transplantation have been used for many years. They evaluate both tumor-initiating and self-renewal capacities and are widely used to assess CSC activity. They have shown that leukemia and many solid tumors are organized along a hierarchical model (18–20). Orthotopic breast cancer xenografts have been shown to keep the features of their corresponding human tumors and to predict prognosis in patients (21). Yet, the validity of xenotransplant assays for CSC studies has been questioned. The use of highly immunodeficient mice increases the frequency of tumorigenic cells in certain types of cancers such as melanoma (22, 23). Furthermore, this model tests the potential of cells to form tumors, not their actual fate in the tumor in which they are born, regardless of microenvironmental variables. Notwithstanding these issues, the CSC model suggests that focusing attention and therapies on CSCs rather than on non-CSCs may improve prognosis and help cure cancer. However, both the clinical relevance and universality of the CSC model remain to be firmly established in solid tumors. An approach would be to show that features of CSCs, but not of non-CSCs, influence clinical outcome. A recent study has shown emerging evidence supports the idea that properties of leukemic stem cells (LSC) may be associated with prognosis (24). Here, we report the establishment of a bank of patient-derived xenografts (PDX) from primary breast cancer (xenobank). We found that a xenograft retains the main features of its cognate primary tumor and that successful

Authors' Affiliations: [1]INSERM, U1068, CRCM, Molecular Oncology, [2]Institut Paoli-Calmettes, Biopathology, [3]Aix-Marseille Univ, UM 105, F-13284, Départements [4]d'Oncologie Médicale, [5]Chirugie oncologique, and [6]Radiologie, Institut Paoli-Calmettes, Marseille; and [7]Plateforme ARN interference PArl, CEA SACLAY, Gif-sur-Yvette, France

Note: Supplementary data for this article are available at Cancer Research Online (http://cancerres.aacrjournals.org/).

Corresponding Author: Emmanuelle Charafe-Jauffret, Centre de Recherche en Cancérologie de Marseille (CRCM), Départements d'Oncologie Moléculaire et de Pathologie, 232, Bd de Ste Marguerite, Marseille 13009, France. Phone: 33-491223457; Fax: 33-491223544; E-mail: jauffrete@ipc.unicancer.fr

doi: 10.1158/0008-5472.CAN-12-4704

engraftment is correlated with the presence of CSCs in the primary tumor and predicts prognosis in patients. We established the gene expression signatures (GES) of functionally validated CSC populations (breast CSC-GES) and tested their clinical relevance in patients with breast cancers. This functionally validated CSC population is correlated with survival and expresses genes governing stem cell functions, supporting a major prediction of the CSC model and opening further promises for new anti-CSC therapies using valid preclinical models.

Materials and Methods

Ethics statement

Samples of human origin and associated data were obtained from the IPC/CRCM Tumour Bank that operates under authorization # AC-2007-33 granted by the French Ministry of Research. Before scientific use of samples and data, patients were appropriately informed and asked to consent in writing, in compliance with French and European regulations. The project was approved by the IPC Institutional Review Board. Animal studies were approved by the INSERM office for Laboratory Animal Medicine.

Primary tumor samples

All tissue samples were collected prospectively at the Institut Paoli-Calmettes from January 2008 to June 2009. Samples were obtained from fresh entire core biopsies or surgical specimen. Tumoral cells content was evaluated under light microscope: when it reached at least 70% of cells, the sample was selected for study and for one part frozen in liquid nitrogen and for another part directly processed for mice implantation. All the histoclinical information of 74 different samples collected are listed in Supplementary Table S1. Patient's treatments followed the standard guidelines of our institute: 56 patients underwent anthracyclin-based chemotherapy, 59 irradiation, and 41 received hormone therapy.

Primary tumor processing and implantation

Human breast primary tumors obtained after surgery were dissociated mechanically and enzymatically using collagenase/hyaluronidase (StemCell Technologies) digestion to generate single-cell suspension for the *in vivo* implantation. For each primary tumor dissociated, 1×10^6 cells were implanted orthotopically in humanized cleared fat pads of NSG (NOD/Shi-scid/IL-2Rγnull) mice for establishing xenotransplants as previously described (Supplementary Information; ref. 19).

Flow cytometric analysis

The analysis was processed on single-cell suspension from our PDXs obtained as described above. ALDEFLUOR kit (StemCell Technologies) was used to isolate the population with high ALDH enzymatic activity as previously described (19). To eliminate cells of mouse origin from the PDXs, we used staining with an anti-H2Kd antibody (BD Biosciences, 1:200, 20 minutes on ice) followed by staining with a secondary antibody labeled with phycoerythrin (PE; Jackson Laboratories, 1:250, 20 minutes on ice).

Tumorigenicity assay

We evaluate the outgrowth potential of each population (ALDEFLUOR-positive, ALDEFLUOR-negative, unselected) sorted from three different PDXs (CRCM226 x, CRCM174 x, CRCM168 x) and injected in cleared humanized fat pads of NSG mice. We conducted serial passages *in vivo*, using limiting dilutions of ALDEFLUOR-positive, -negative, and unselected cells (50,000 cells; 5,000 cells; 3,000 cells; 500 cells; 300 cells). For each PDX model and for each limiting dilutions, 10 fat pads were injected. Each tumors generated with 500 sorted cells were serially re-implanted three times and in 10 different fat pads. Each mouse that present a tumor reaching a size of 10 mm was considered as a tumor-bearing mouse.

Immunohistochemistry

Expression of ALDH1, CD44/CD24, ER, ERBB2, Ki67, PR, and p53 was studied by immunohistochemistry. The characteristics of the antibodies and experimental procedures are described in the Supplementary Information.

DNA and RNA extraction

DNA and RNA were extracted from frozen primary tumor samples, PDXs, and ALDEFLUOR-positive/-negative cells by using the All prep DNA/RNA/Protein Mini Kit (Qiagen) for primary tumors and PDXs and the RNeasy Micro Kit (Qiagen) for ALDEFLUOR-sorted cells.

Gene expression analysis

Gene expression profiling was done with Affymetrix U133 Plus 2.0 human oligonucleotide microarrays. Preparation of cRNA, hybridizations, washes, and detection were done as previously described (25). See Supplementary Information for further detailed description of gene expression array and bioinformatics analysis.

Array comparative genomic hybridization analysis

Array-based comparative genomic hybridization (array-CGH) was applied to 75 samples (53 primary tumors and 22 PDXs, including 19 early passages and 3 late passages) using high-resolution 244 K CGH microarrays (Hu-244A, Agilent Technologies). See Supplementary Information for further detailed description of gene expression array and bioinformatics analysis.

siRNA screen and ALDEFLUOR analysis

We use the SUM159 mesenchymal breast cancer cell line (BCL) and S68 luminal BCL to conduct the siRNA screen. The cell lines were grown using the recommended culture conditions (26). We have adapted a methodology to optimize the reverse transfection of SUM159 and S68 cells using Lipofectamine RNAiMAX (Invitrogen). Five thousand cells were plated in triplicate in 96-well plates with 0.25 pmol of siRNA in 25 μL of Opti-MEM I Medium. The ALDEFLUOR-positive population was evaluated in triplicate at 72 hours after lipofection. We have validated that CSCs and nontumorigenic cells were equally transfected (data not shown). We miniaturized the ALDEFLUOR assay for CSC-enriched population detection per cell in 96-well plate. For each well, we used 0.25 μL of substrate (BAAA) and 100 μL of ALDEFLUOR buffer. We used an

automated fluorescence-activated cell sorting (FACS; LSR2) to detect the ALDEFLUOR-positive population in each well. Each experiment was controlled in 6-plicate using cells incubated with 0.5 μL of DEAB. The mini siRNA library of 19 genes was designed by Qiagen based on a published library siRNA that have been shown in peer-reviewed publication to provide effective gene silencing. We used 3 siRNAs per selected gene, most likely in triplicates and considered as a "hit" each siRNA construct that induces a variation of the number of ALDEFLUOR-positive cells over a threshold of 2-fold the CSC proportion detected in the control (BCLs infected with a MOCK siRNA). Cell viability was evaluated using 4′,6-diamidino-2-phenylindole (DAPI) staining.

siRNA screen and sphere formation efficiency analysis

We have conducted the siRNA screen with both BCLs following the reverse transfection protocol described before. Then, 72 hours after lipofection, BCLs were dissociated and plated as single cells in ultra-low attachment plates (Corning, www.sigmaaldrich.com) at low density (1,000 viable cells per milliliter). Cells were grown as previously described (27). After 5 days of suspension culture, the capacity of cells to form tumor spheres was quantified.

Statistical analysis

Statistical analyses used the SPSS software (version 10.0.5) and are described in Supplementary Information.

Results

Generation of PDXs

We transplanted 74 fresh primary breast tumors from 71 different individuals into cleared and humanized mammary fat pads of female NSG mice. All implanted tumors were from primary tumor and not from metastasis. The 74 primary tumors implanted cover the main histoclinical features met in an unselected set of breast tumors (Supplementary Table S1). Twenty PDXs were established of the 74 primary samples transplanted with an engraftment rate of 27%. We successfully maintained 13 PDXs through serial passages (transplantable rate: 17.5%); 7 were lost between the first and the fourth passages. The average delay of growth of PDXs was 212 days (range, 77–466). PDX growth kinetic (time to reach 10 mm) was stable or accelerated with serial passages (Supplementary Fig. S1).

PDXs maintain the histologic and phenotypic features of primary tumors

We compared histology, Scarff-Bloom-Richardson (SBR) grade, and pathologic phenotype (based on ERBB2, ER, PR, Ki67, p53 protein expression) of PDXs with those of the cognate primary tumors. We observed a striking preservation of the main histological (Fig. 1A and B) and immunohistochemical features (Table 1). Among the 20 PDXs, only the expression of hormonal receptors [estrogen receptor (ER) and/or progesterone receptor (PR)] was lost in 4 PDXs of 11 compared with their corresponding primary tumors. ERBB2 overexpression or "triple-negative" phenotype was maintained in all the PDXs. All the primary tumors that successfully engraft presented a high grade (SBR grade ≥ 2), which was retained in PDXs. Concerning p53 status, only one discordant case (CRCM274) was observed with a gain of p53 overexpression in the PDXs.

PDXs maintain the genome profile and retain the molecular subtype of cognate primary tumors

In 18 paired primary tumors/PDXs, we determined the genomic profiles according to DNA copy number alterations (CNA; Supplementary Fig. S2). We observed an almost perfect preservation of the genomic profiles in paired PDXs with a correlation score of 0.81 (Fig. 1D). Furthermore, late passages in mice (CRCM168 X P11, CRCM226 X P10, CRCM237 X P8) preserved a genomic profile identical to early passages (P0 to P2; Fig. 1D). We profiled 19 paired primary tumors/PDXs using Affymetrix whole-genome oligonucleotide microarrays and determined the molecular subtypes by using the PAM50 predictor. Primary tumors from the 5 major molecular subtypes successfully engraft with 1 luminal A, 4 luminal B, 4 ERBB2-like, 8 basal, and 2 normal-like. In 14 pairs of 19, the molecular subtype of the PDXs was identical to that of the corresponding primary tumor (Fig. 1C). CRCM214 PT and CRCM274 PT were respectively of luminal B and luminal A subtypes, but their paired PDXs lost expression of ER or PR and switched to an ERBB2 subtype, without modification of ERBB2 expression. CRCM184 X and CRCM272 X were respectively of ERBB2 and luminal B subtype, whereas the parental primary tumors were of normal-like subtype; this is likely to be due to the dilution of ERBB2- or ER-overexpressing cancer cells by abundant stromal and normal breast tissue in the human samples (Supplementary Fig. S3). Thus, our model of xenografts generally phenocopied the major molecular features of the corresponding primary tumors and maintained these features among passages.

PDXs present a hierarchical organization driven by a CSC population

To evaluate the presence of a CSC population in our PDXs, we used the ALDEFLUOR assay. We detected an ALDEFLUOR-positive population in all tested xenografts, ranging from 0.2% to 12.3% (average 3.88%) of the total cancer cell population (Supplementary Fig. S4). ALDEFLUOR-positive and -negative cells isolated from 3 different PDXs were transplanted in limited dilutions in recipient mice. The percentage of tumor-bearing mice decreased with the number of injected ALDEFLUOR-negative cells from 77% with 50,000 ALDEFLUOR-negative cells to 0% with 300 ALDEFLUOR-negative cells, whereas 100% of mice injected with ALDEFLUOR-positive cells developed tumors, even with 300 cells only (Fig. 2A). The breast CSC frequency as determined by limiting dilution analysis (LDA) *in vivo* was higher in the ALDEFLUOR-positive cell population [1:1; confidence interval (CI), 1–697] than in the ALDEFLUOR-negative cell population (1:14,038; CI, 7,007–28,126; $P = 2.13e{-}18$) or the unselected cell population (1:1572; CI, 880–2,806; $P = 3.08e{-}06$; Supplementary Table S2). Moreover, tumor growth rates were higher in tumors generated from ALDEFLUOR-positive population than in tumors generated from ALDEFLUOR-negative or unsorted populations (Fig. 2B, Supplementary Fig. S5). Furthermore, only ALDEFLUOR-positive cells were able to regenerate both ALDEFLUOR-positive and -negative cells along passages,

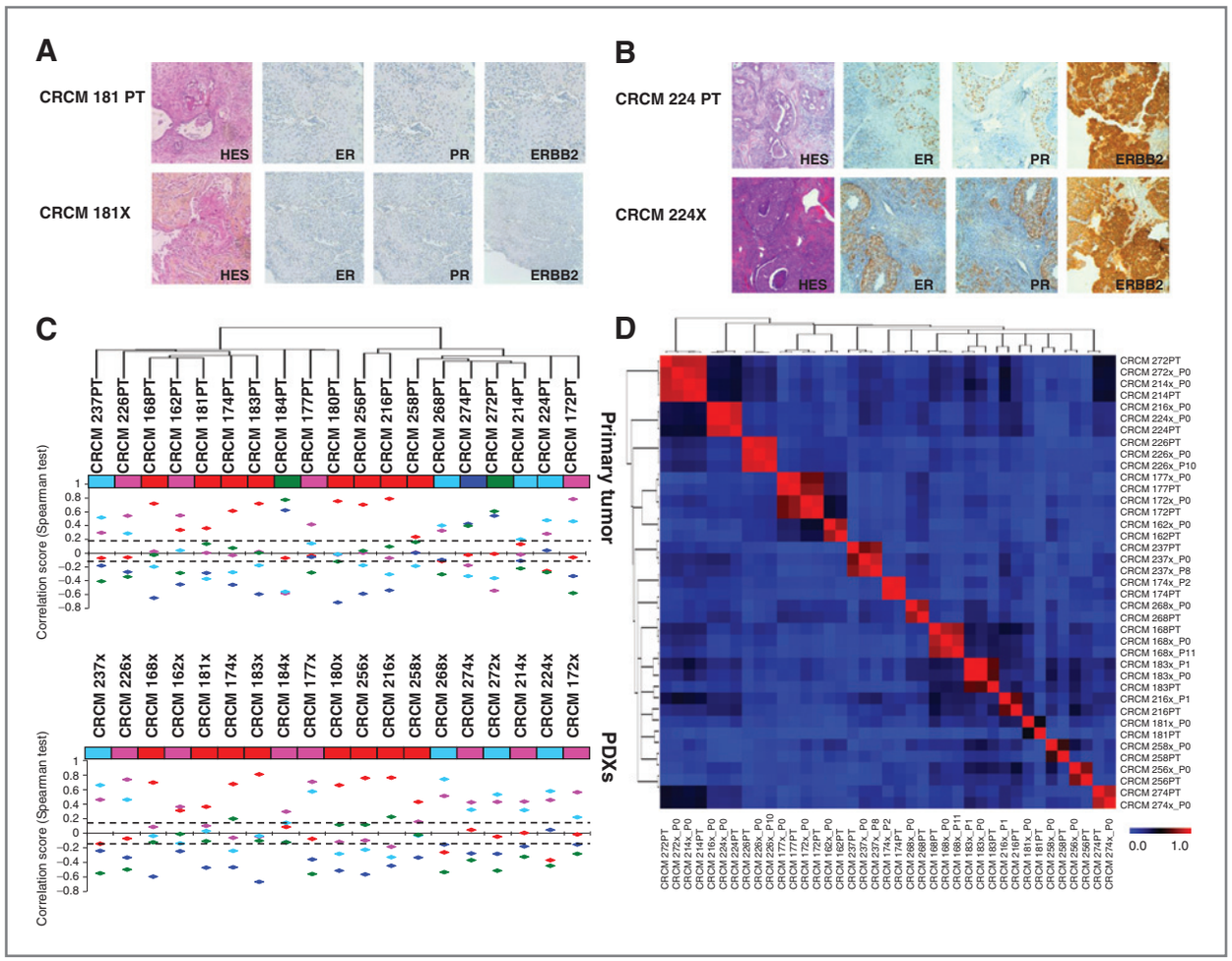

Figure 1. PDXs resemble the primary tumors from which they are derived. A and B, histology of two paired primary tumors/PDXs: CRCM181, a triple-negative metaplastic breast cancer (A), and CRCM224, a luminal B breast cancer (B). Histology evaluated after hematoxylin and eosin staining and immunohistochemical staining for ER, PR, and ERBB2 protein expression are strictly conserved in PDXs. C, correlation of gene expression of the 19 paired primary tumors (top)/PDXs (bottom) to 5 molecular subtypes defined by the PAM50 predictor. For each subtype, a median profile is defined and compared with the sample's median profile. Correlation coefficients are plotted by colors indicating the subtype: dark blue, luminal A; light blue, luminal B; red, basal; pink, ERBB2-like; and green, normal-like. The dashed line, the threshold for correlation coefficient significance (0.15). D, correlation matrix evaluating the genomic profile similarity between primary tumors and PDXs. Each sample (19 pairs and 3 late-passage PDXs) is classified according to their genomic profile similarities (Spearman test). Correlation coefficient are depicted according to the color scale, with blue for a correlation coefficient null meaning an absence of correlation, and red for a correlation coefficient equal to 1 meaning a perfect correlation.

showing that they are able to self-renew and differentiate (Fig. 2C). The tumorigenic potential of the ALDEFLUOR-negative population was lost with passages, whereas it was maintained in the ALDEFLUOR-positive population, suggesting that the ALDEFLUOR-negative population contains cells that have proliferation potential but lack self-renewal ability (Fig. 2D). Thus, our PDXs retained a hierarchical organization with an ALDEFLUOR-positive CSC population that initiates and maintains tumor growth.

Histologic grade and ALDH1-positive CSC content of primary tumors predict engraftment

The clinical relevance of PDX models is suggested by the good correlation between success in engraftment and survival of patients (21). In our series, we thus first questioned whether engraftment was associated with clinical outcome. Only 4% of primary tumors that failed to engraft versus 34% of primary tumors that did developed metastasis within the first 3 years of follow-up (log-rank test, $P = 0.003$; Fig. 2E). Moreover, among the different histoclinical parameters associated with metastasis-free survival (MFS), only positive axillary lymph node (pN) and primary tumor engraftment were independent factors associated with MFS (Supplementary Fig. S6). This observation confirms that primary tumor engraftment is strongly correlated with disease evolution. However, the factors that influence tumor engraftment are not known. In our series, engraftment was not correlated with the type of sample (core biopsy or surgical sample) used for primary injection (Supplementary Fig. S7). Among the different histoclinical and molecular factors tested (Supplementary Fig. S8), engraftment was

Table 1. Histoclinical data for primary tumors and corresponding PDXs

Primary tumors								PDXs							
ID	Histologic type	Grade SBR	ER status	PR status	ERBB2 status	Ki67 status	p53 status	ID	Histologic type	Grade SBR	ER status	PR status	ERBB2 status	Ki67 status	p53 status
CRCM162 PT	IDC	3	Positive	Negative	Positive	Positive	Negative	CRCM162 X	IDC	3	Positive	Negative	Positive	Positive	Negative
CRCM168 PT	IDC	3	Positive	Positive	Negative	Positive	Negative	CRCM168 X	IDC	3	Negative	Negative	Negative	Positive	Negative
CRCM172 PT	IDC	3	Positive	Negative	Positive	Negative	Negative	CRCM172 X	IDC	3	Negative	Negative	Positive	Negative	Negative
CRCM174 PT	IDC	3	Negative	Negative	Negative	Negative	Positive	CRCM174 X	IDC	3	Negative	Negative	Negative	Positive	Positive
CRCM177 PT	IDC	3	Positive	Negative	Positive	Negative	Positive	CRCM177 X	IDC	3	Positive	Negative	Positive	Positive	Heterogeneous
CRCM180 PT	IDC	3	Negative	Negative	Negative	Positive	Negative	CRCM180 X	IDC	3	Negative	Negative	Negative	Positive	Negative
CRCM181 PT	MED	2	Negative	Negative	Negative	Positive	Negative	CRCM181 X	MED	2	Negative	Negative	Negative	Positive	Negative
CRCM183 PT	IDC	3	Negative	Negative	Negative	Positive	Heterogeneous	CRCM183 X	IDC	3	Negative	Negative	Negative	Positive	Heterogeneous
CRCM184 PT	IDC	3	Negative	Negative	Positive	Negative	Positive	CRCM184 X	IDC	3	Negative	Negative	Positive	Negative	Positive
CRCM214 PT	IDC	3	Positive	Positive	Negative	Positive	Negative	CRCM214 X	IDC	3	Positive	Negative	Negative	Negative	Negative
CRCM216 PT	IDC	3	Negative	Negative	Negative	Positive	Heterogeneous	CRCM216 X	IDC	3	Negative	Negative	Negative	Positive	Negative
CRCM224 PT	IDC	3	Positive	Positive	Positive	Positive	Heterogeneous	CRCM224 X	IDC	3	Positive	Positive	Positive	Positive	Heterogeneous
CRCM226 PT	IDC	2	Negative	Negative	Positive	Positive	Positive	CRCM226 X	IDC	2	Negative	Negative	Positive	Negative	Positive
CRCM236 PT	IDC	3	Positive	Positive	Positive	Negative	Positive	CRCM236 X	IDC	3	Negative	Negative	Positive	Negative	Positive
CRCM237 PT	IDC	3	Positive	Positive	Positive	Positive	Negative	CRCM237 X	IDC	3	Positive	Positive	Positive	Positive	Negative
CRCM256 PT	CS	3	Negative	Negative	Negative	Positive	Negative	CRCM256 X	CS	3	Negative	Negative	Negative	Positive	Negative
CRCM258 PT	IDC	2	Negative	Negative	Negative	Negative	Positive	CRCM258 X	IDC	2	Negative	Negative	Negative	Negative	Positive
CRCM268 PT	IDC	3	Positive	Positive	Positive	Negative	Negative	CRCM268 X	IDC	3	Positive	Positive	Positive	Positive	Negative
CRCM272 PT	IDC	2	Positive	Positive	Negative	Negative	Negative	CRCM272 X	IDC	2	Positive	Negative	Negative	Negative	Negative
CRCM274 PT	IDC	3	Positive	Positive	Negative	Negative	Negative	CRCM274 X	IDC	3	Negative	Positive	Negative	Negative	Positive

NOTE: Heterogeneous, <70% of positive cells.

Abbreviations: IDC, invasive ductal carcinoma; MED, medullary breast carcinoma; CS, carcinosarcoma.

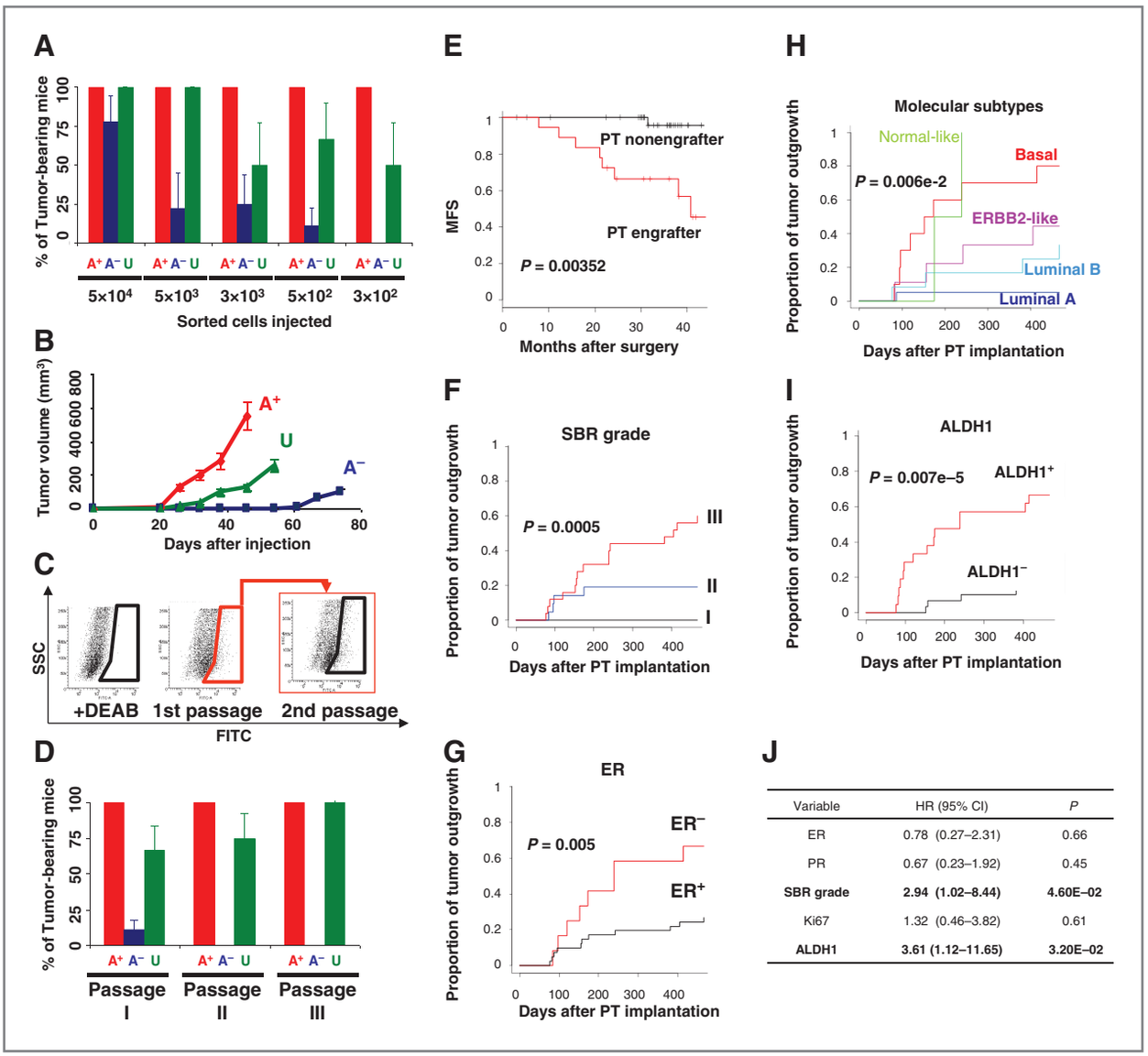

Variable	HR (95% CI)	*P*
ER	0.78 (0.27–2.31)	0.66
PR	0.67 (0.23–1.92)	0.45
SBR grade	**2.94 (1.02–8.44)**	**4.60E–02**
Ki67	1.32 (0.46–3.82)	0.61
ALDH1	**3.61 (1.12–11.65)**	**3.20E–02**

Figure 2. ALDH1-CSCs drive tumorigenicity in PDXs and predict primary tumor engraftment. A–D, the outgrowth potential of sorted populations (ALDEFLUOR-positive, A^+; ALDEFLUOR-negative, A^-; unselected, U) from three independent PDXs (CRCM226 x, CRCM168 x, and CRCM174 x) was evaluated, revealing a limited potential of the ALDEFLUOR-negative population, whereas ALDEFLUOR-positive cells generated tumors in all fat pads injected even with only 300 cells (A). An example of outgrowth kinetic is represented in B for CRCM226 x and an injection of 300 sorted cells. Outgrowth kinetics for all PDX models and all limited dilutions are represented in Supplementary Fig. S5. For each PDX model tested, the ALDEFLUOR-positive population recreated the native cellular heterogeneity and gave rise to ALDEFLUOR-positive and -negative cells, as shown in C for CRCM168 x (similar results were observed for CRCM226 x and CRCM174 x). The outgrowth potential of the ALDEFLUOR-positive population was maintained within three serial passages, whereas it was lost at passage 2 for the ALDEFLUOR-negative population (D). Data represent mean ± SD. E, successful engraftment of primary tumor specimens predicts metastasis formation in patients (log-rank test, $P = 0.00352$). A Kaplan–Meier MFS analysis shows patient's outcome in engrafter and nonengrafter groups. F–I, factors predicting successful engraftment in mice. Kaplan–Meier analysis shows proportion of tumor outgrowth for different groups of primary tumor injected and stratified according to SBR grade, ER protein expression, molecular subtypes, or the presence of ALDH1-positive cells. Each of these factors identifies different groups of primary tumor with opposite engraftment rate. J, multivariate analysis with Cox proportional model identifies only SBR grade and ALDH1 expression as independent factors associated with successful engraftment.

associated with high SBR grade ($P = 0.0005$), absence of ER expression ($P = 0.005$), high proliferation rate ($P = 0.003$), and molecular subtype ($P = 0.006$; Fig. 2F and G and Supplementary Fig. S6). Interestingly, within a molecular subtype, the engraftment rate perfectly matched the clinical outcome associated (Fig. 2H). In contrast, no recurrent genomic alteration was associated with engraftment (Supplementary Fig. S9). We next tested whether the expression of CSC markers (ALDH1, $CD44^+/CD24^-$) in primary tumors was correlated with engraftment. Of the 69 primary tumors injected and analyzed for ALDH1 expression, 24 had ALDH1-positive cells. We observed only 5 ALDH1-positive tumors in the 45 (11%) nonengrafters, whereas

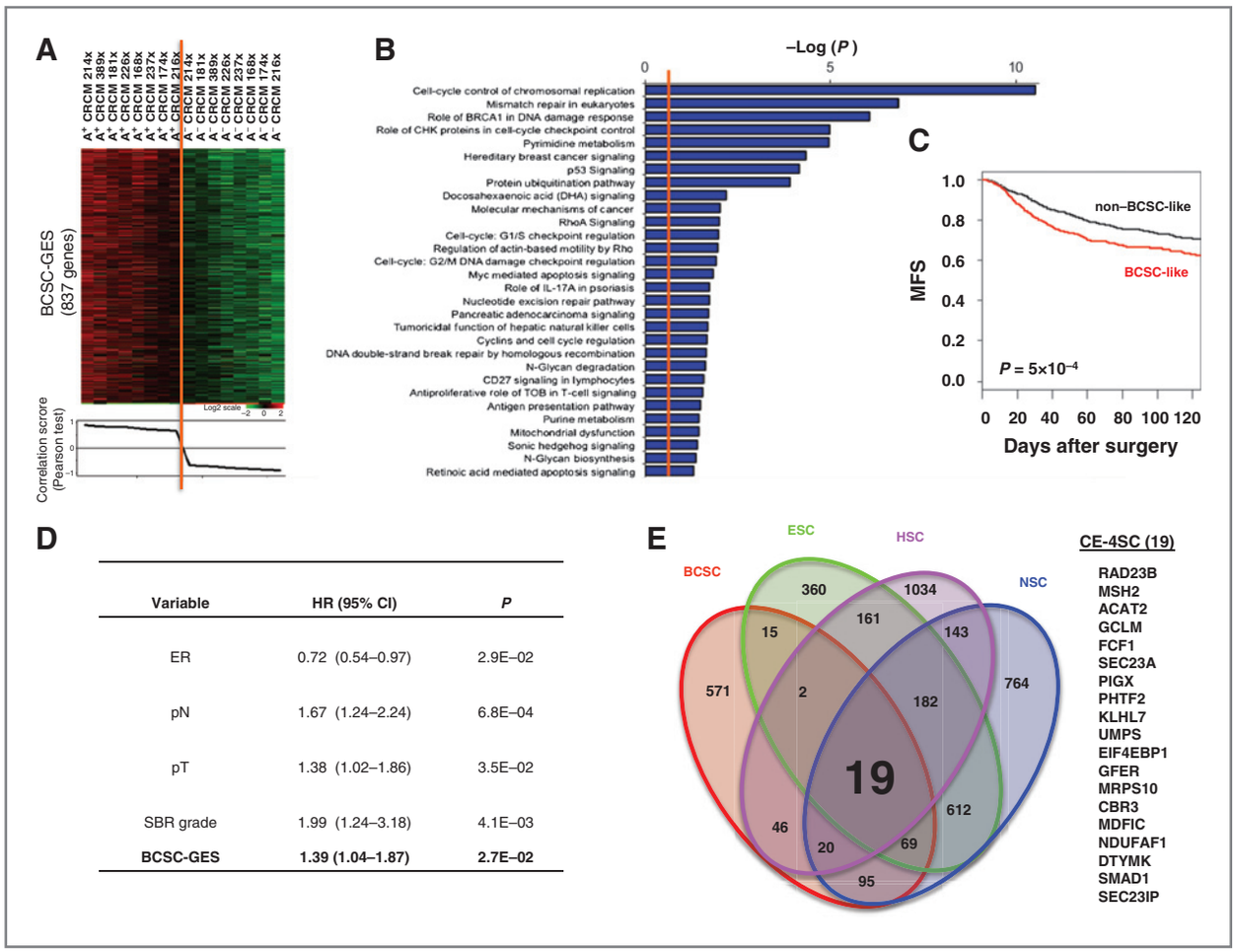

Figure 3. Identification of a "common" stem cell core transcriptional program (CE-4SC) associated with clinical outcome. A, supervised analysis identified a breast BCSC-GES. Gene expression profiles of ALDEFLUOR-positive and -negative populations, isolated from 5 PDXs, were compared: 837 genes were identified as differentially expressed between CSCs and non-CSCs and are represented on hierarchical clustering. B, to determine the pathways associated with the BCSC-GES, we ran Ingenuity Pathway Analysis using Ingenuity software. Bar plot represents enrichment for each of the network components identified, where the strength of the association is represented by the −log (*P*). C, Kaplan–Meier MFS curves according to BCSC-GES status. Tumors that express the BCSC-GES (BCSC-like) are associated with a reduced MFS ($P = 5.10 - 4$). D, multivariate analysis with Cox proportional model identified BCSC-GES as independent factor associated with MFS. E, identification of a "universal" stem cell core transcriptional program corresponding to the common 19 genes of 4 stemness GES. The overlap of the 4 GES is represented with a Venn diagram. The 19 common genes (named CE-4SC) are listed.

15 of the 20 (75%) engrafters were ALDH1-positive ($P = 7.2e{-}5$; Fig. 2I). In contrast, the presence of $CD44^{+}/CD24^{-}$ cells in primary tumors was not associated with engraftment (Supplementary Fig. S6). Using multivariate analysis with Cox proportional model, only SBR grade and ALDH1 expression were independent factors associated with successful engraftment (Fig. 2J). These results confirm the correlation between patient's outcome, the capacity for a primary tumor to be xenografted, and the presence of ALDH1-positive CSCs. They further suggest that the molecular machinery governing CSC properties is likely to influence clinical outcome.

Transcriptional profiles of CSCs isolated from PDXs

To identify molecular networks regulating CSC biology, we used Affymetrix microarrays to establish the gene expression profiles of sorted ALDEFLUOR-positive and -negative populations from 8 different PDXs. Significance Analysis of Microarrays analysis identified 837 genes as differentially expressed [false discovery rate (FDR) = 0.05]—hereafter designated as the breast CSC gene expression signature (BCSC-GES)—between the ALDEFLUOR-positive and -negative populations (Fig. 3A, Supplementary Table S3). To determine whether genes overexpressed in ALDEFLUOR-positive cells were commonly enriched in known corresponding signaling pathways, we ran a gene ontology analysis (Fig. 3B and Supplementary Table S4). Among the different pathways identified, several play a role in stem cell biology (BRCA1, p53, SHH, and retinoic pathways), supporting the potential stem cell nature of our BCSC-GES. The remaining pathways were associated with 2 main cell functions (Supplementary Figs. S10 and S11): cell-cycle control and especially the G_1–S checkpoint controlling a crucial step for cell fate decision (28) and DNA damage repair.

BCSC-GES is associated with poor prognosis in breast cancer

We studied the correlation between the BCSC-GES and histoclinical data using 13 clinically annotated gene expression data sets corresponding to 2,609 patients (Supplementary Table S5). On the basis of the BCSC-GES, the samples were classified as "BCSC-like" (1,443 samples) or "non–BCSC-like" (1,196 samples). Correlations were found between these two classes and all histoclinical features except patient's age and histological type: as compared with "non–BCSC-like" samples, "BCSC-like" samples were more frequently SBR grade 3, with a TNBC (triple-negative breast cancer) phenotype and axillary lymph node metastasis (Table S6). The prognostic value regarding MFS was tested within the 1,642 patients with available follow-up (8 of 13 datasets). The 5-year MFS rate was 70% (95% CI, 67–74) in the "BCSC-like" group and 80% (95% CI, 77–83) in the "non–BCSC-like" group ($P = 5.5e{-}04$, log-rank test; Fig. 3C). In multivariate analysis, all these variables remained significant, including the BCSC-GES–based classification ($P = 0.027$; HR, 1.39; 95% CI, 1.04–1.87; Fig. 3D), suggesting that our BCSC-GES determined in our PDXs was independently associated with prognosis in primary breast cancer.

Identification of a "common" stem cell core transcriptional program

To gain insight into the molecular mechanisms that govern stem cell intrinsic functions, we searched for common expression patterns between our 837-gene BCSC-GES and 3 stemness GES defined from embryonic, neural, and hematopoietic stem cells (29). Enrichment test was significant with each of the tested stemness GES and the core stemness GES (3SC) defined by Ramalho-Santos and colleagues (Supplementary Table SV7). In contrast, no enrichment was found between our BCSC-GES and the 65-gene signature identified to be upregulated in differentiated cells. A total of 19 genes were common to the 4 stem cell signatures (BCSC, ESC, HSC, NSC; Fig. 3E). These leading genes were called the core-enriched 4SC genes (CE-4SC). We then derived a metagene classifier based on the combined expression of these 19 genes and determined its prognostic relevance in our public data set of 1,642 patients with breast cancer. On the basis of the metagene, 2 classes of patients were defined and associated with different MFS (Supplementary Fig. S12): the CE-4SC–positive class (733 patients) displayed a 67% 5-year MFS rate (95% CI, 64–71) and the CE-4SC–negative class (909 patients) displayed an 81% 5-year MFS rate (95% CI, 78–83; $P = 4.8E{-}06$, log-rank test). In multivariate analysis, the CE-4SC signature kept its independent prognostic value (Supplementary Fig. S12). Collectively, these data indicate that our "common" stem cell transcriptional program influences patient outcome and represent a short list of genes to identify key CSC regulators.

The "common" stem cell core transcriptional program functionally regulates CSC self-renewal and differentiation

Overall, the 19 CE-4SC genes are poorly characterized but might be preferentially active in CSCs as compared with the bulk of tumor cells and represent candidates for CSC targeting. Using the SUM159 mesenchymal BCL, we conducted a screening of an RNA interference library specially designed to block the expression of these 19 genes. We used 3 independent siRNA sequences per gene (57 siRNA constructs) and evaluated the effect of single gene knockdown (KD) on the breast CSC population using a miniaturized ALDEFLUOR assay in 96-well plates. Among the 19 genes, the knockdown of 14 genes significantly modified the ratio CSC/non-CSC (Fig. 4A). Within these 14 genes, 2 groups were identified. In the first group of 5 genes (*ACAT2*, *CBR3*, *DTYMK*, *NDUFAF1*, *PHTF2*), the CSC population decreased when gene expression was knocked down. Conversely, in the second group of 10 genes (*ACAT2*, *FCF1*, *GFER*, *GCLM*, *KLHL7*, *MDFIC*, *MRPS10*, *MSH2*, *RAD23B*, *UMPS*), the CSC population significantly increased. To validate this observation, we tested the effect of the 57 siRNAs on tumor sphere formation efficiency (SFE). SFE is an *in vitro* assay used as a surrogate method to evaluate the proportion of CSCs. We observed a strong correlation between modification of the ALDEFLUOR-positive/ALDEFLUOR-negative ratio and the SFE after gene knockdown ($\rho = 0.826$; CI, 0.72–0.89; $P = 4.4e{-}15$; Fig. 4B). To confirm these results, we screened our siRNA library using the luminal BCL S68. We observed similar results in the two BCLs analyzed ($P = 0.003$), with 13 of 19 genes with comparable effect after the gene knockdown on the ALDEFLUOR-positive population (Supplementary Fig. S13). We never observed an opposite effect of a specific gene knockdown in the 2 BCLs and only 5 genes (*EIF4EBP1*, *FCF1*, *GCLM*, *KLHL7*, *SEC23IP*) presented a restricted effect in one BCL when gene expression was knocked down. The results on the ALDEFLUOR-phenotype obtained in S68 were similarly validated using SFE assay ($\rho = 0.79$; CI, 0.61–0.87; $P = 6.3e{-}10$; Supplementary Fig. S14). These results represent a first validation of the functional role of our CE-4SC signature in the regulation of breast CSC biology with genes that may be implicated either in self-renewal program or in differentiation process.

Discussion

We established a bank of serially transplantable, orthotopic xenografts of primary breast cancers in humanized mouse fat pad. The PDXs maintained the main histologic, phenotypical, and molecular features of the cognate primary tumors as shown before in other PDX models (21, 30). We show that the xenografts maintain the same hierarchical organization as the primary tumors, with CSCs able to self-renew and differentiate. Our findings have 3 important implications for breast cancer understanding and treatment.

First, our study contributes to the definition of CSCs. As pointed out in the report of "The Year 2011 Working Conference on CSCs," despite the deep clinical implications of the CSC model, CSC investigation has been hampered both by a lack of consistency in the terms used for these cells and by how they are defined (31). Whereas the phenotypic definition ($CD44^{+}/CD24^{-/low}$ or ALDEFLUOR-positive cells for breast CSCs) can restrain the population to a subset of CSCs, a functional definition based on tumor-initiating or tumor-maintaining properties seems more appropriate. Xenograft assays outlined

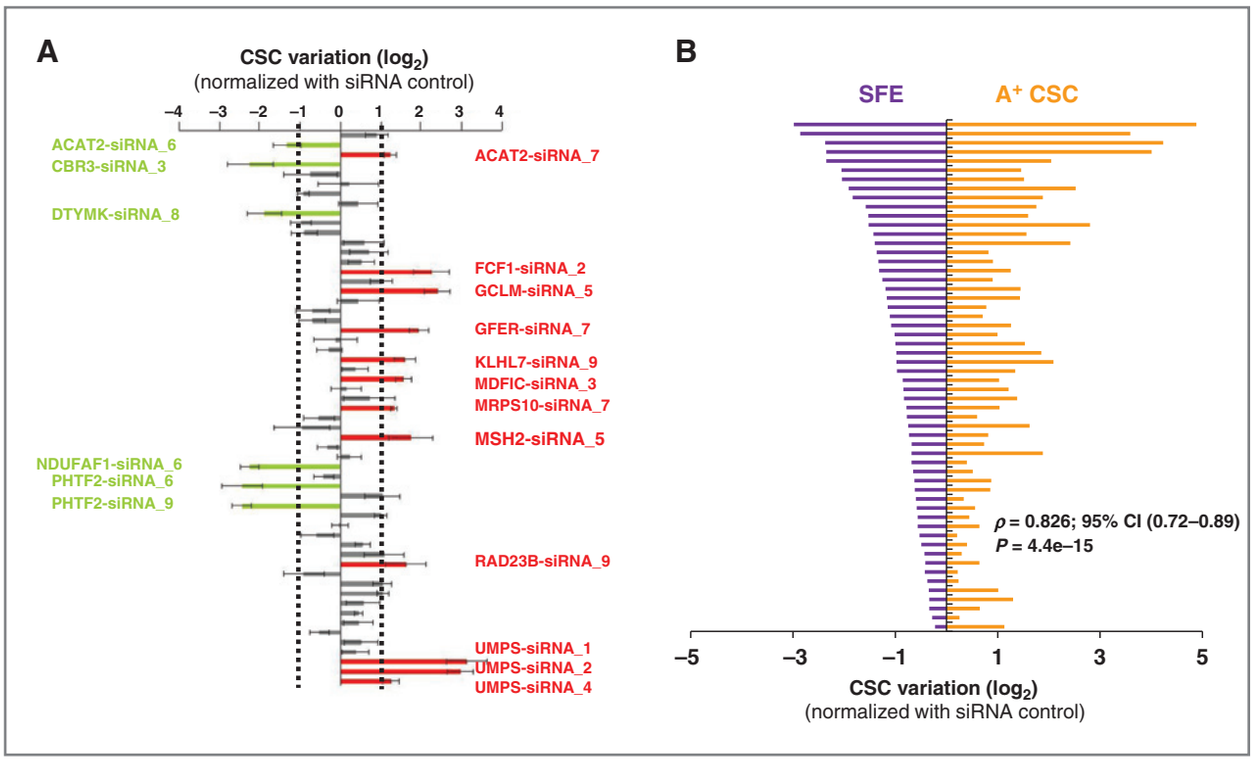

Figure 4. Functional validation of the CE-4SC using siRNAs screen in SUM159 BCL. A, screening of a library of 57 siRNAs targeting the 19 identified genes using the variation of the ALDEFLUOR-positive population as read out. Each siRNA construct that induced a variation in the number of ALDEFLUOR-positive cells over a threshold of 2-fold the CSC proportion detected in the control was considered as a hit. Eighteen hits were identified, corresponding to 14 unique genes, with green siRNA constructs that reduced significantly the CSC population and red siRNA constructs that increased significantly the CSC population. B, comparison of CSC variation after gene knockdown by ALDEFLUOR phenotyping (right) and tumor SFE (left) using the 57 siRNAs. Results for each siRNA (from top to bottom) are represented as opposite bars. Correlations are measured using Spearman rank correlation (ρ). Data represent mean ± SD.

a population of cells in an operational rather than in a conceptual context, based on tumor-initiating or tumor-maintaining properties, recapitulation of the entire tumoral heterogeneity. The paradigm of xenograft assay as a gold standard to evaluate CSC activity has also been challenged as the ability of a subpopulation of tumor cells to generate a tumor in the mouse might reflect the permissivity of these cells for a specific environment (22, 32). In that context, we questioned the clinical relevance of the xenograft assay. We showed that primary breast tumors that generate PDXs have more ALDH1-positive cells (CSCs) and are more prone to form metastasis in patients than tumors that failed to graft. We showed that tumor engraftment is an independent prognostic factor, as strong as lymph node invasion to predict metastasis. Our study establishes a direct link between primary tumor engraftment, functionally defined breast CSCs, and patient's clinical outcome, suggesting that CSCs are not artifacts of the experimental PDX model but reflect intrinsic tumor biology.

Second, we show that the molecular machinery that governs CSCs is clinically relevant. This crucial issue has been shown in acute myeloid leukemia, where a functionally defined LSC or HSC signature is correlated with disease outcome (24). In breast, an "invasiveness" gene signature generated by comparing $CD44^+/CD24^{-/low}$ breast cancer cells with that of normal breast epithelium is associated with disease outcome (33) and a $CD44^+$ cell signature that contains stem cell markers is correlated with decreased survival in patients (34). Furthermore, a normal mammary stem cell signature predicts breast cancer biologic and molecular features, and high-grade tumors contain more CSCs than low-grade tumors (35). Yet, the potential link between functionally defined CSCs and engraftment has never been described so far. This approach provides a paradigm for assessing both the identity and clinical relevance of CSCs from breast cancer and other solid tumors. Importantly, because our findings support CSC clinical relevance, it suggests that therapies targeting CSCs would improve survival outcome and that xenograft models based on primary breast CSC engraftment can be crucial in the preclinical evaluation of new cancer drugs.

Third, the identification of shared transcriptional profiles in CSCs and ESC/HSC/NSC suggests that common genes have a role in establishing and maintaining the stem cell state and that these shared determinants of stemness influence clinical outcome. We identified a "common" stem cell core transcriptional program. This core of genes common to 4 stem cell gene expression signatures contains genes implicated in oxidative phosphorylation, detoxification, lipid metabolism, and genomic stability. Some of these genes encode drug resistance enzymes (UMPS; ref. 36) or cell-cycle regulators through P27 function (GFER; refs. 37, 38). Metabolic alterations in tumor

cells are thought to be important for the tumor phenotype and evolution and to affect response to therapy (39). In embryonic, neural, normal, and tumoral breast tissues, stem/progenitor cells contain lower level of reactive oxygen species than their more mature progeny, sustaining their relative resistance to radiation (40, 41). In leukemia, oxidative phosphorylation triggers genomic instability and is a putative mechanism explaining relapse after tyrosine kinase inhibitor treatment (42, 43). Noteworthy, aldehyde dehydrogenase, a hallmark of embryonic, normal adult tissue and CSCs, oxidizes aldehydes to the corresponding carboxylic acids (44). Furthermore, we recently identified the importance of mevalonate metabolism in the P27-dependent regulation of breast CSCs (45). Our findings reinforce recent literature data and suggest that metabolic therapies anti-CSCs might be a new therapeutic approach to cure cancer. These novel results however need further validation.

In the opening era of personalized medicine, targeting the cell subpopulation that sustains tumor growth and development could help design new therapeutic strategies to cure cancer. In breast cancer, use of PDXs that mimic human tumor is increasing to capture tumor heterogeneity and elaborate the best therapeutic strategy for patients (46, 47). The clinical relevance of PDXs studies for CSCs in breast cancer suggests that this model is reliable to test anti-CSC therapies. If confirmed, our data indicate the importance of developing CSC biomarkers and will move forward a new era of accelerated transfer for personalized cancer therapy into clinics.

Disclosure of Potential Conflicts of Interest

No potential conflicts of interest were disclosed.

Authors' Contributions

Conception and design: E. Charafe-Jauffret, C. Ginestier, D. Birnbaum
Development of methodology: E. Charafe-Jauffret, C. Ginestier, O. Cabaud, J. Wicinski, E. Josselin, T.-T. Nguyen, F. Monville, G. Pinna, A. Harel-Bellan
Acquisition of data (provided animals, acquired and managed patients, provided facilities, etc.): C. Ginestier, F. Bertucci, O. Cabaud, J. Wicinski, P. Finetti, E. Josselin, J. Adelaide, T.-T. Nguyen, J. Jacquemier, G. Pinna, E. Lambaudie, G. Houvenaeghel, P. Viens
Analysis and interpretation of data (e.g., statistical analysis, biostatistics, computational analysis): E. Charafe-Jauffret, C. Ginestier, F. Bertucci, J. Wicinski, P. Finetti, G. Pinna, M. Chaffanet, D. Birnbaum
Writing, review, and/or revision of the manuscript: E. Charafe-Jauffret, C. Ginestier, F. Bertucci, G. Houvenaeghel, M. Chaffanet, D. Birnbaum
Administrative, technical, or material support (i.e., reporting or organizing data, constructing databases): O. Cabaud, P. Finetti, E. Josselin, J. Adelaide, G. Pinna, G. Houvenaeghel, I. Xerri, P. Viens
Study supervision: E. Charafe-Jauffret, D. Birnbaum

Acknowledgments

The authors thank CRCM Centre de Ressources Biologiques CRB (C. Chabannon) for tissue conservation and providing, CRCM animal core facility for animal housing, CRCM flow cytometry core, Xentech company, Evry France (J.G. Judde) for helpful technical discussions. They also thank J.-P. Borg for discussions and encouragements and to CIML flow cytometry core (M. Malissen and P. Grenot) for the technical assistance. They also thank the support of FEDER for the purchase of the ARIA III cell sorter. This work is dedicated to the memory of Rémy Galindo.

Grant Support

This work is supported by INSERM, Institut Paoli-Calmettes, Institut National du Cancer-DGOS grant TRANSLA11-103 (E. Charafe-Jauffret), and Ligue Nationale Contre le Cancer Label DB (D. Birnbaum) grant INCa-DGOS-Inserm 6038.

The costs of publication of this article were defrayed in part by the payment of page charges. This article must therefore be hereby marked *advertisement* in accordance with 18 U.S.C. Section 1734 solely to indicate this fact.

Received January 6, 2013; revised August 13, 2013; accepted September 9, 2013; published OnlineFirst October 18, 2013.

References

1. Shackleton M, Quintana E, Fearon ER, Morrison SJ. Heterogeneity in cancer: cancer stem cells versus clonal evolution. Cell 2009;138:822–9.
2. Charafe-Jauffret E, Monville F, Ginestier C, Dontu G, Birnbaum D, Wicha MS. Cancer stem cells in breast: current opinion and future challenges. Pathobiology 2008;75:75–84.
3. Kakarala M, Wicha MS. Implications of the cancer stem-cell hypothesis for breast cancer prevention and therapy. J Clin Oncol 2008;26:2813–20.
4. Pajonk F, Vlashi E, McBride WH. Radiation resistance of cancer stem cells: the 4 R's of radiobiology revisited. Stem Cells 2010;28:639–48.
5. Phillips TM, McBride WH, Pajonk F. The response of CD24(−/low)/CD44 +breast cancer-initiating cells to radiation. J Natl Cancer Inst 2006;98:1777–85.
6. Reya T, Morrison SJ, Clarke MF, Weissman IL. Stem cells, cancer, and cancer stem cells. Nature 2001;414:105–11.
7. Visvader JE, Lindeman GJ. Stem cells and cancer - the promise and puzzles. Mol Oncol 2010;4:369–72.
8. Ishizawa K, Rasheed ZA, Karisch R, Wang Q, Kowalski J, Susky E, et al. Tumor-initiating cells are rare in many human tumors. Cell Stem Cell 2010;7:279–82.
9. Korkaya H, Wicha MS. Selective targeting of cancer stem cells: a new concept in cancer therapeutics. BioDrugs 2007;21:299–310.
10. Korkaya H, Wicha MS. Cancer stem cells: nature versus nurture. Nat Cell Biol 2010;12:419–21.
11. Liu S, Wicha MS. Targeting breast cancer stem cells. J Clin Oncol 2010;28:4006–12.
12. Anderson K, Lutz C, van Delft FW, Bateman CM, Guo Y, Colman SM, et al. Genetic variegation of clonal architecture and propagating cells in leukaemia. Nature 2011;469:356–61.
13. Gibbs KD Jr, Jager A, Crespo O, Goltsev Y, Trejo A, Richard CE, et al. Decoupling of tumor-initiating activity from stable immunophenotype in HoxA9- Meis1-driven AML. Cell Stem Cell 2012;10:210–7.
14. Visvader JE, Lindeman GJ. Cancer stem cells: current status and evolving complexities. Cell Stem Cell 2012;10:717–28.
15. Chen J, Li Y, Yu TS, McKay RM, Burns DK, Kernie SG, et al. A restricted cell population propagates glioblastoma growth after chemotherapy. Nature 2012;488:522–6.
16. Driessens G, Beck B, Caauwe A, Simons BD, Blanpain C. Defining the mode of tumour growth by clonal analysis. Nature 2012;488:527–30.
17. Friedmann-Morvinski D, Bushong EA, Ke E, Soda Y, Marumoto T, Singer O, et al. Dedifferentiation of neurons and astrocytes by oncogenes can induce gliomas in mice. Science 2012;338:1080–4.
18. Bonnet D, Dick JE. Human acute myeloid leukemia is organized as a hierarchy that originates from a primitive hematopoietic cell. Nat Med 1997;3:730–7.
19. Ginestier C, Hur MH, Charafe-Jauffret E, Monville F, Dutcher J, Brown M, et al. ALDH1 is a marker of normal and malignant human mammary stem cells and a predictor of poor clinical outcome. Cell Stem Cell 2007;1:555–67.
20. Ricci-Vitiani L, Lombardi DG, Pilozzi E, Biffoni M, Todaro M, Peschle C, et al. Identification and expansion of human colon-cancer-initiating cells. Nature 2007;445:111–5.
21. DeRose YS, Wang G, Lin YC, Bernard PS, Buys SS, Ebbert MT, et al. Tumor grafts derived from women with breast cancer authentically

reflect tumor pathology, growth, metastasis and disease outcomes. Nat Med 2011;17:1514–20.
22. Quintana E, Shackleton M, Sabel MS, Fullen DR, Johnson TM, Morrison SJ. Efficient tumour formation by single human melanoma cells. Nature 2008;456:593–8.
23. Quintana E, Shackleton M, Foster HR, Fullen DR, Sabel MS, Johnson TM, et al. Phenotypic heterogeneity among tumorigenic melanoma cells from patients that is reversible and not hierarchically organized. Cancer Cell 2010;18:510–23.
24. Eppert K, Takenaka K, Lechman ER, Waldron L, Nilsson B, van GP, et al. Stem cell gene expression programs influence clinical outcome in human leukemia. Nat Med 2011;17:1086–93.
25. Bertucci F, Finetti P, Cervera N, Charafe-Jauffret E, Buttarelli M, Jacquemier J, et al. How different are luminal A and basal breast cancers? Int J Cancer 2009;124:1338–48.
26. Charafe-Jauffret E, Ginestier C, Monville F, Finetti P, Adelaide J, Cervera N, et al. Gene expression profiling of breast cell lines identifies potential new basal markers. Oncogene 2006;25:2273–84.
27. Charafe-Jauffret E, Ginestier C, Iovino F, Wicinski J, Cervera N, Finetti P, et al. Breast cancer cell lines contain functional cancer stem cells with metastatic capacity and a distinct molecular signature. Cancer Res 2009;69:1302–13.
28. Orford KW, Scadden DT. Deconstructing stem cell self-renewal: genetic insights into cell-cycle regulation. Nat Rev Genet 2008;9:115–28.
29. Ramalho-Santos M, Yoon S, Matsuzaki Y, Mulligan RC, Melton DA. "Stemness": transcriptional profiling of embryonic and adult stem cells. Science 2002;298:597–600.
30. Marangoni E, Vincent-Salomon A, Auger N, Degeorges A, Assayag F, de CP, et al. A new model of patient tumor-derived breast cancer xenografts for preclinical assays. Clin Cancer Res 2007;13:3989–98.
31. Valent P, Bonnet D, De MR, Lapidot T, Copland M, Melo JV, et al. Cancer stem cell definitions and terminology: the devil is in the details. Nat Rev Cancer 2012;12:767–75.
32. Kelly PN, Dakic A, Adams JM, Nutt SL, Strasser A. Tumor growth need not be driven by rare cancer stem cells. Science 2007;317:337.
33. Liu R, Wang X, Chen GY, Dalerba P, Gurney A, Hoey T, et al. The prognostic role of a gene signature from tumorigenic breast-cancer cells. N Engl J Med 2007;356:217–26.
34. Shipitsin M, Campbell LL, Argani P, Weremowicz S, Bloushtain-Qimron N, Yao J, et al. Molecular definition of breast tumor heterogeneity. Cancer Cell 2007;11:259–73.
35. Pece S, Tosoni D, Confalonieri S, Mazzarol G, Vecchi M, Ronzoni S, et al. Biological and molecular heterogeneity of breast cancers correlates with their cancer stem cell content. Cell 2010;140:62–73.
36. Muhale FA, Wetmore BA, Thomas RS, McLeod HL. Systems pharmacology assessment of the 5-fluorouracil pathway. Pharmacogenomics 2011;12:341–50.
37. Sankar U, Means AR. Gfer is a critical regulator of HSC proliferation. Cell Cycle 2011;10:2263–8.
38. Teng EC, Todd LR, Ribar TJ, Lento W, Dimascio L, Means AR, et al. Gfer inhibits Jab1-mediated degradation of p27kip1 to restrict proliferation of hematopoietic stem cells. Mol Biol Cell 2011;22:1312–20.
39. Cairns RA, Harris IS, Mak TW. Regulation of cancer cell metabolism. Nat Rev Cancer 2011;11:85–95.
40. Diehn M, Cho RW, Lobo NA, Kalisky T, Dorie MJ, Kulp AN, et al. Association of reactive oxygen species levels and radioresistance in cancer stem cells. Nature 2009;458:780–3.
41. Diehn M, Clarke MF. Cancer stem cells and radiotherapy: new insights into tumor radioresistance. J Natl Cancer Inst 2006;98:1755–7.
42. Flis K, Irvine D, Copland M, Bhatia R, Skorski T. Chronic myeloid leukemia stem cells display alterations in expression of genes involved in oxidative phosphorylation. Leuk Lymphoma 2012;53:2474–8.
43. Nieborowska-Skorska M, Kopinski PK, Ray R, Hoser G, Ngaba D, Flis S, et al. Rac2-MRC-cIII-generated ROS cause genomic instability in chronic myeloid leukemia stem cells and primitive progenitors. Blood 2012;119:4253–63.
44. Muzio G, Maggiora M, Paiuzzi E, Oraldi M, Canuto RA. Aldehyde dehydrogenases and cell proliferation. Free Radic Biol Med 2012;52:735–46.
45. Ginestier C, Monville F, Wicinski J, Cabaud O, Cervera N, Josselin E, et al. Mevalonate metabolism regulates Basal breast cancer stem cells and is a potential therapeutic target. Stem Cells 2012;30:1327–37.
46. Siolas D, Hannon GJ. Patient derived tumor xenografts: transforming clinical samples into mouse models. Cancer Res 2013;73:5315–9.
47. Zhang X, Claerhout S, Prat A, Dobrolecki L, Petrovic I, Lai Q, et al. A renewable tissue resource of phenotypically stable, biologically and ethnically diverse, patient-derived human breast cancer xenografts. Cancer Res 2013;73:4885–97.